Electronic Supplementary Material (ESI) for Sustainable Energy & Fuels.


# Graphene and graphene-cellulose nanocrystals composite films for sustainable anodes in biophotovoltaic devices

Sara Lund*[,a,b,c], Laura T. Wey*[,c], Jouko Peltonen[a], Johan Bobacka[a,b], Rose-Marie-Latonen[†,a,b], Yagut Allahverdiyeva[†,c]

[a] Laboratory of Molecular Science and Engineering, Faculty of Science and Engineering, Åbo Akademi University, Henriksgatan 2, 20500 Turku (Åbo), Finland

[b] Johan Gadolin Process Chemistry Centre (PCC), Åbo Akademi University, Henriksgatan 2, 20500 Turku (Åbo), Finland

[c] Photomicrobes Research Group, Molecular Plant Biology unit, Department of Life Technologies, University of Turku, 20014 Turku, Finland.

*These authors contributed equally: Sara Lund, Laura T. Wey

[†]Corresponding authors: allahve@utu.fi, rose-marie.latonen@abo.fi

# Supplementary Information

**Table S1** A comparison of graphene-based electrodes in three-electrode biophotovoltaic systems. PSII = photosystem II, 2,6-dichloro-1,4-benzoquinone = DCBQ**,** IO **=** inverse opal, RGO = reduced graphene oxide, ITO = indium tin oxide, PEI = polyethyleneimine, TM = thylakoid membrane, GC = glassy carbon, PAH = polyallylamine hydrochloride, PEN = polyethylene naphthalate, CNC = cellulose nanocrystals, * = co-assembled with the biocatalyst. The current at 0.6 V vs SHE using the graphene anode was recorded during the stepped chronoamperometry measurement (Fig. S5) which was not done with the graphene-CNC electrode.

| **Biocatalyst** | **Artificial electron mediator** | **Electrode material** | **Electrode structure** | **Reducing agents** | **Applied Bias Potential (V vs SHE)** | **Photocurrent (μA cm$^{-2}$)** | **Year** | **Ref.** |
|---|---|---|---|---|---|---|---|---|
| **PSII** | DCBQ | IO-RGO on ITO | 3D | Reduced by annealing at 500 °C | 0.5 | 0.44 ± 0.02 (no artificial mediator) 4.19 ± 0.01 (artificial mediator) | 2019 | [1] |
| **PSII** | No | PEI-RGO* on ITO | Layered | Hydrazine | 0.49 | 0.0372 | 2015 | [2] |
| **TM** | No | Aminoaryl func. RGO on GC | Porous/3D, planar microstructure | Electroreduction | 0.6 | 5.24 ± 0.50 | 2018 | [3] |
| **TM** | 1.5 mM $K_4[Fe(CN)_6]$ | GO / RGO* on ITO | Flat | PAH, hydrazine | 0.44 | 21.37 ± 1.11 / 18.95 ± 0.54 | 2018 | [4] |
| **TM** | 10 mM $K_3[Fe(CN)_6]$ | GO* on ITO-PEN | Flat | Not reduced | 0.64 | 3.92 | 2019 | [5] |
| ***Synechocystis*** | 1.0 mM $K_3[Fe(CN)_6]$ | Graphene | Rough | No | 0.70 (Fig. 4B) | 2.17 ± 0.74 | 2023 | This work |
| ***Synechocystis*** | 1.0 mM $K_3[Fe(CN)_6]$ | Graphene-CNC (thick) | Rough | No | 0.70 (Fig. 4B) | 1.11 ± 0.60 | 2023 | This work |
| ***Synechocystis*** | 1.0 mM $K_3[Fe(CN)_6]$ | Graphene-CNC (thin) | Rough | No | 0.70 (Fig. 4B) | 0.60 ± 0.12 | 2023 | This work |
| ***Synechocystis*** | No | Graphene | Rough | No | 0.60 (Fig. S5) | 0.058 ± 0.018 | 2023 | This work |

**Table S2** A comparison of graphene-based electrodes in two-electrode biophotovoltaic systems. RGO = reduced graphene oxide, $TiO_2$ = titanium dioxide, CC = carbon cloth.

| Biocatalyst | Artificial electron mediator | Anode material | Anode structure | Max. power output (mW $m^{-2}$) | Year | Ref. |
|---|---|---|---|---|---|---|
| ***Chlorella* sp. *(UMACC 313)*** | NA | RGO on glass | Porous | 0.27 (dark background not subtracted) | 2014 | [6] |
| ***Chlorella* sp. (UMACC 313)** | NA | RGO on glass | Rough | $6.935 \times 10^8$ (dark background not subtracted) | 2017 | [7] |
| ***Synechococcus elongatus*** | NA | RGO on glass | NA | 0.538 ± 0.014 | 2018 | [8] |
| ***Chlorella vulgaris*** | No | $TiO_2$/RGO on CC | Fibrous | 34.66 ± 1.3 | 2018 | [9] |

**Table S3** Surface roughness parameters of graphene and graphene-CNC films determined from 5.0 µm × 5.0 µm AFM images. Data presented as mean **±** standard deviation (n = 3 films, 3 images /per film). The parameters are Root-mean-square (RMS)-roughness ($S_q$), ten-point height ($S_{10z}$), skewness ($S_{sk}$), kurtosis ($S_{ku}$), density of summits ($S_{ds}$) and effective surface area ($S_{dr}$).

| Film material | $S_q$ (nm) | $S_{10z}$ (nm) | $S_{sk}$ | $S_{ku}$ | $S_{ds}$ (µ$m^{-2}$) | $S_{dr}$ (%) |
|---|---|---|---|---|---|---|
| **Graphene** | 44.1 ± 13.4 | 238 ± 76 | 0.2 ± 0.3 | 3.3 ± 0.4 | 29.0 ± 6.7 | 1.6 ± 1.3 |
| **Graphene-CNC** | 40.8 ± 3.2 | 334 ± 21 | -0.1 ± 0.2 | 3.5 ± 0.1 | 163.5 ± 21.3 | 16.6 ± 0.7 |

**Table S4** The anodic and cathodic peak currents ($I_{p,a}$ and $I_{p,c}$) and potentials ($E_{p,a}$ and $E_{p,c}$), and the peak separation ($\Delta E_p$) for different replicates of graphene and graphene-CNC electrodes spray-coated on non-conductive glass measured in 1.0 M $KNO_3$ electrolyte with either 0.5 mM $K_3[Fe(CN)_6]$ and 0.5 mM $K_4[Fe(CN)]_6$ or 1.0 mM $[Ru(NH_3)_6]Cl_3$ with a scan rate of 50 mV $s^{-1}$. Dispersion volumes of 2.5 ml and 2.0 ml were used for spray-coating the thick and thin electrodes, respectively.

| Electrode | $I_{p,a}$ (mA $cm^{-2}$) | $E_{p,a}$ (V) | $I_{p,c}$ (mA $cm^{-2}$) | $E_{p,c}$ (V) | $\Delta E_p$ (V) | Fig. No |
|---|---|---|---|---|---|---|
| **Graphene with $Fe(CN)_6^{3-/4-}$** | 0.13 | 0.33 | -0.15 | 0.24 | 0.090 | 2B |
| **Graphene-CNC with $Fe(CN)_6^{3-/4-}$** | 0.13 | 0.40 | -0.12 | 0.19 | 0.21 | 2B |
| **ITO with $Fe(CN)_6^{3-/4-}$** | 0.12 | 0.32 | -0.12 | 0.23 | 0.091 | 2B |
| | | | | | | |
| **Graphene with $Ru(NH_3)_6^{3+}$** | 0.14 | -0.14 | -0.24 | -0.24 | 0.10 | S2 |
| **Graphene-CNC with $Ru(NH_3)_6^{3+}$** | 0.11 | -0.051 | -0.086 | -0.30 | 0.25 | S2 |
| | | | | | | |
| **Graphene-CNC (thin) with $Fe(CN)_6^{3-/4-}$** | 0.11 | 0.38 | -0.11 | 0.185 | 0.20 | S6 |
| **Graphene-CNC (thick) with $Fe(CN)_6^{3-/4-}$** | 0.11 | 0.37 | -0.093 | 0.200 | 0.18 | S6 |
| | | | | | | |
| **Graphene (thin) with $Fe(CN)_6^{3-/4-}$** | 0.17 | 0.32 | -0.17 | 0.23 | 0.090 | S6 |
| **Graphene (thick) with $Fe(CN)_6^{3-/4-}$** | 0.13 | 0.33 | -0.15 | 0.23 | 0.095 | S6 |

**Table S5** The average thicknesses, conductivities and sheet resistance ranges of graphene and graphene-CNC films. Thicknesses and conductivities presented as mean **±** standard deviation (graphene and thick graphene-CNC: n = 4, thin graphene-CNC: n = 3). The sheet resistances are calculated for the same films and given as a range from the smallest to the largest value.

| Film type | Film thickness (nm) | Film conductivity (S $m^{-1}$) | Sheet resistance (Ω/sq) |
|---|---|---|---|
| **Graphene** | 760 ± 100 | 8 900 ± 1 300 | 130 - 170 |
| **Graphene-CNC (thick)** | 1590 ± 460 | 1 500 ± 400 | 270 - 790 |
| **Graphene-CNC (thin)** | 880 ± 140 | Not measured | |

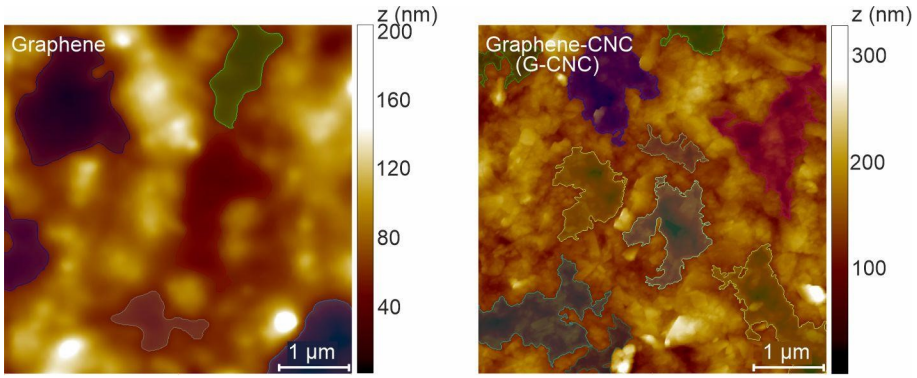


**Fig. S1** Top-view topographical atomic force micrograms of graphene (on the left) and graphene-CNC (on the right) films on glass. Scale bar 1 µm indicates x-y plane; whole image is 5.0 µm x 5.0 µm; colour scale bar on right indicates z-height. The coloured areas in the images boundary cavities.

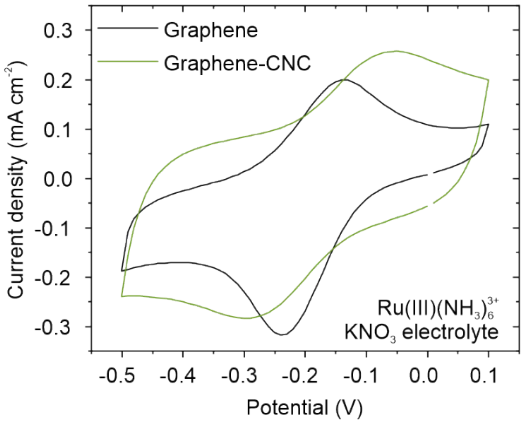


**Fig. S2** Cyclic voltammograms of the graphene (black) and graphene-CNC (green) films on non-conductive glass in 1.0 mM $[Ru(NH_3)_6]Cl_3$ and 1.0 M $KNO_3$ as the background electrolyte. Scan rate 50 mV $s^{-1}$. The last cycle of five cycles is shown. The scanning direction which applies for all CVs is indicated with an arrow in Fig. 2A. The starting potential was 0.0 V.

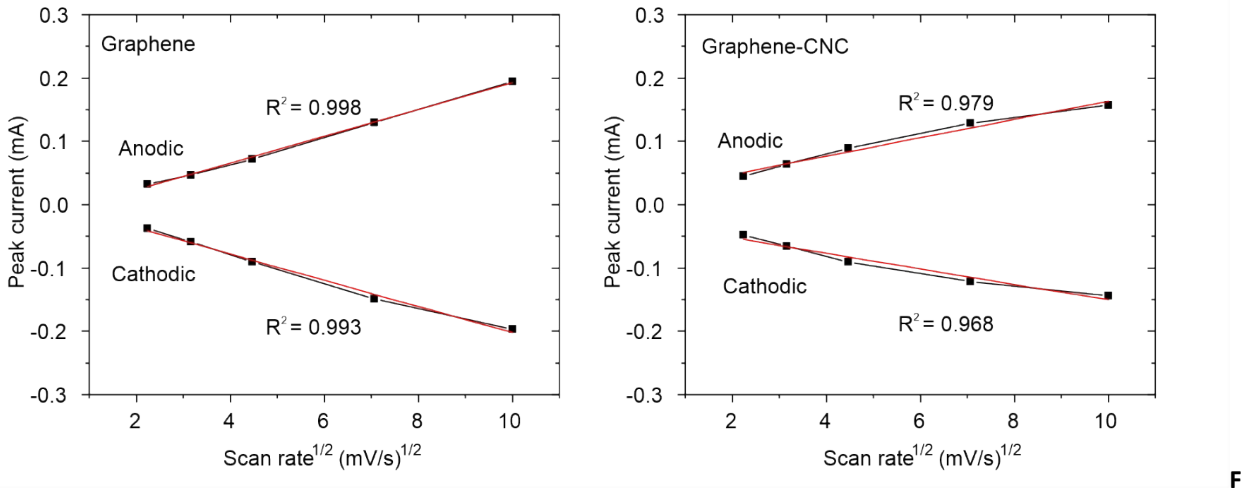


**Fig. S3** The anodic and the cathodic peak currents as a function of the square roots of the scan rates of graphene (on the left) and graphene-CNC (on the right) films in 0.5 mM $K_3[Fe(CN)_6]$, 0.5 mM $K_4[Fe(CN)_6]$ and 1.0 M $KNO_3$ measured with scan rates of 5, 10, 20, 50 and 100 mV $s^{-1}$.

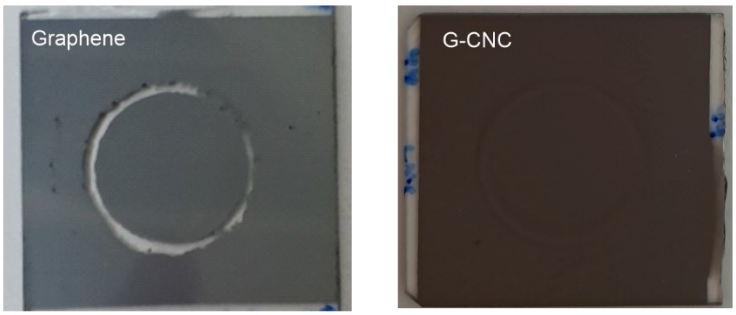


**Fig. S4** Photos of graphene and graphene-CNC films on glass substrate after cyclic voltammetry experiments were performed in BG11 (pH 8.2) electrolyte and photoelectrochemical apparatus was disassembled.

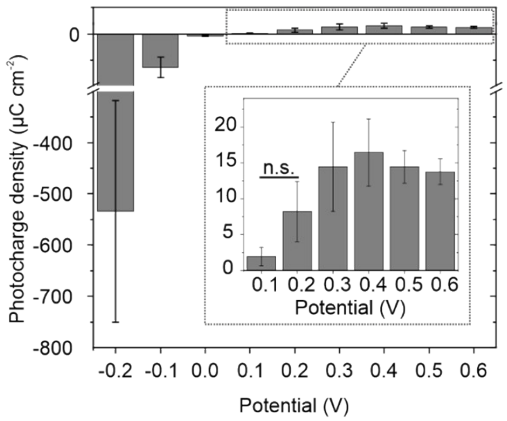


**Fig. S5** Photocharge density of cyanobacterial cells on graphene anodes at different applied potentials (V vs Ag/AgCl) in BG11 (pH 8.2) electrolyte with 60 nmol Chl a loading and 17 h biofilm formation. The data was recorded under 5/5 min light/dark cycles with light intensity 100 $\mu mol_{photons}\ m^{-2}\ s^{-1}$ and wavelength 660 nm. Photocharge was calculated as area under the current-time trace in light minus the area in dark, each for 5 min. All photocharges in this study are calculated this way. Data presented as the mean of four biological replicates and the error bars are the standard error of the mean.

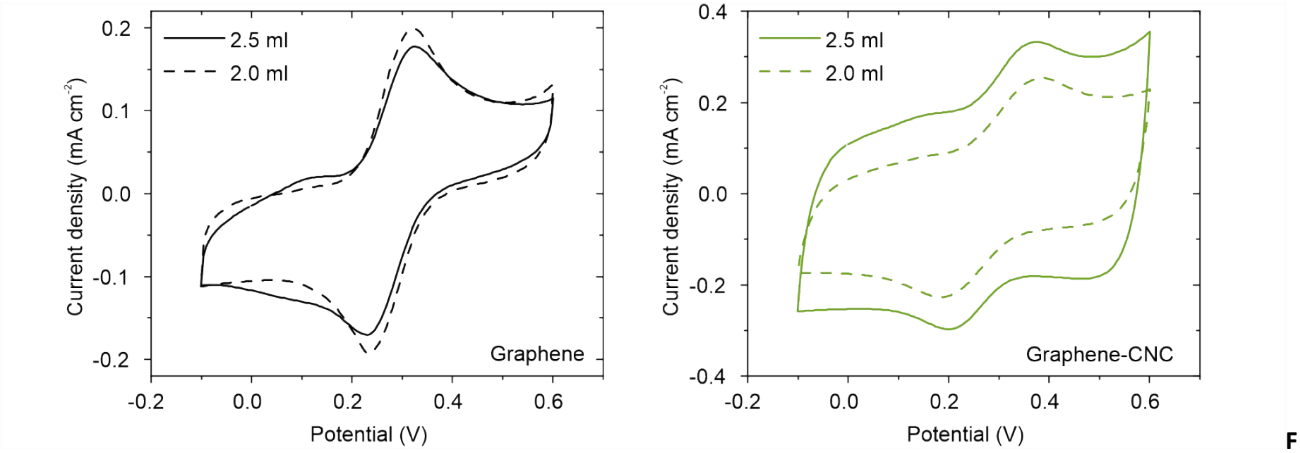


**Figure S6** Cyclic voltammograms of the graphene (on the left) and graphene-CNC (on the right) films with different thicknesses on non-conductive glass in 0.5 mM $K_3[Fe(CN)_6]$ and 0.5 mM $K_4[Fe(CN)_6]$ with 1.0 M $KNO_3$ as the background electrolyte using a scan rate of 50 mV $s^{-1}$. The films of different thicknesses were prepared from the same dispersions using either 2.5 (solid line) or 2.0 ml (dashed line) dispersion volume in spray-coating. The scanning direction which applies for all CVs is indicated with an arrow in Fig. 2A. The starting potential was 0.0 V.

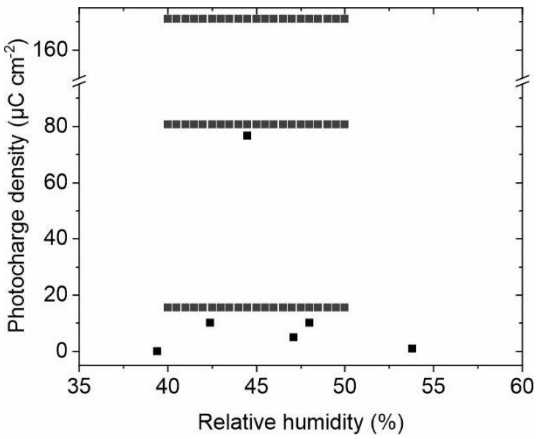


**Fig. S7** Photocharge density of cyanobacterial cells on graphene anodes as a function of relative humidity (RH) with 60 $nmol_{Chl\ a}$ loading and 17 h biofilm formation. The data was recorded under 5/5 min light/dark cycles with light intensity 100 $\mu mol_{photons}\ m^{-2}\ s^{-1}$ and wavelength 660 nm. The dark grey rectangular lines represent the data points where the humidity is estimated to be 40-50% RH. The black squares represent the measured average humidity during the 17 h biofilm incubation.

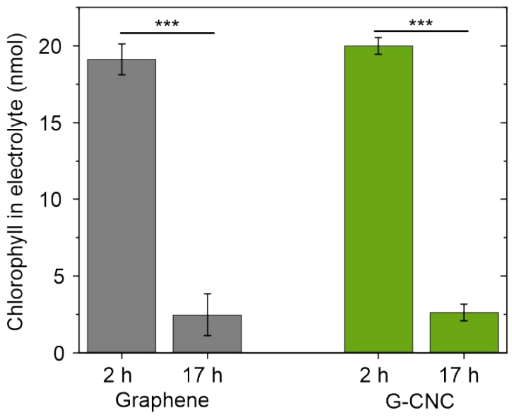


**Fig. S8** Chlorophyll quantification of cyanobacterial cells suspended in the electrolyte after photoelectrochemical experiments after 2 and 17 h biofilm incubation times. Data presented as mean ± standard error of the mean (n = 4 for graphene 2 h, n = 3 for graphene 17 h, n = 2 for G-CNC 2 h and n = 6 for G-CNC 17 h), statistical significance by t-test $P \leq 0.001$ denoted by ***.

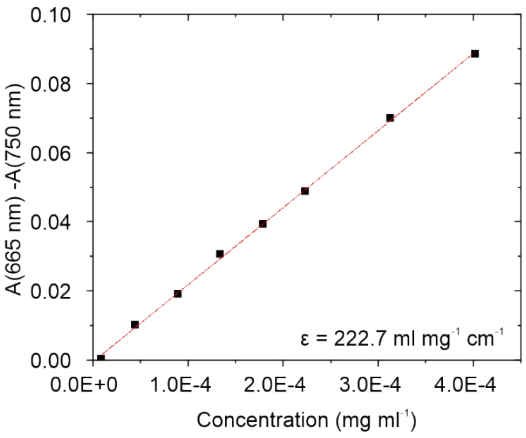


**Fig. S9** Absorbance determined with UV-Vis spectroscopy as a function of Chl *a* concentration in 90 % (v/v) MeOH solution containing also 10% (v/v) electrolyte of BG11 with ferricyanide and DCBQ artificial electron mediator. The extinction coefficient is the slope of the calibration curve.

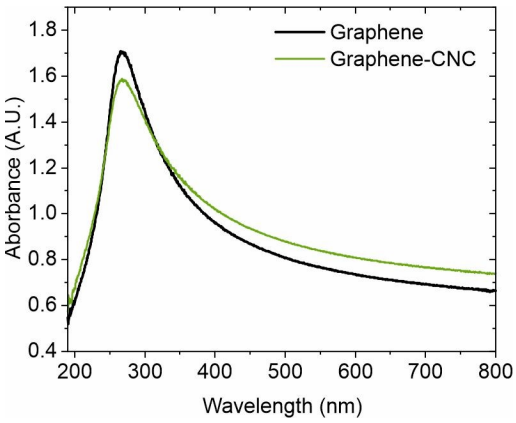


**Fig. S10** Representative UV-vis absorption spectra of graphene and graphene-CNC dispersions showing the typical peak at ca 270 nm corresponding to the π-π* transition of aromatic C-C bonds in graphene.

# References


1. X. Fang, K. P. Sokol, N. Heidary, T. A. Kandiel, J. Z. Zhang and E. Reisner, *Nano Lett.*, 2019, **19**, 1844–1850.
2. P. Cai, X. Feng, J. Fei, G. Li, J. Li, J. Huang and J. Li, *Nanoscale*, 2015, **7**, 10908–10911.
3. G. Pankratova, D. Pankratov, C. Di Bari, A. Goñi-Urtiaga, M. D. Toscano, Q. Chi, M. Pita, L. Gorton and A. L. De Lacey, *ACS Appl. Energy Mater.*, 2018, **1**, 319–323.
4. P. Cai, G. Li, Y. Yang, X. Su and Z. Zhang, *Colloids and Surfaces A: Physicochemical and Engineering Aspects*, 2018, **555**, 37–42.
5. H. Shin, T. Kim, I. Seo, S. Kim, Y. J. Kim, H. Hong, Y. Park, H. M. Jeong, K. Kim and W. Ryu, *Applied Surface Science*, 2019, **481**, 1–9.
6. F.-L. Ng, M. M. Jaafar, S.-M. Phang, Z. Chan, N. A. Salleh, S. Z. Azmi, K. Yunus, A. C. Fisher and V. Periasamy, *Scientific Reports*, 2014, **4**, 7562.
7. S. A. Ibrahim, M. M. Jaafar, F.-L. Ng, S.-M. Phang, G. G. Kumar, W. H. A. Majid and V. Periasamy, *Appl. Phys. A*, 2018, **124**, 59.
8. F.-L. Ng, S.-M. Phang, V. Periasamy, J. Beardall, K. Yunus and A. C. Fisher, *J Appl Phycol*, 2018, **30**, 2981–2988.
9. N. Senthilkumar, S. Sheet, Y. Sathishkumar, Y. S. Lee, S.-M. Phang, V. Periasamy and G. Gnana kumar, *Appl. Phys. A*, 2018, **124**, 769.